CASE REPORT | Article in Press

Therapeutic potential of SAT-3247 in a canine model of Duchenne muscular dystrophy

Shanti S. S. Rayagiri · Johnathan K. Smid · Phil Lambert · James Jaquith · Tessa Murray · Ryan Mitchell · Frank Gleeson · Jacob G. Monast · James A. Teixeira · Yongping Yue · Matthew J. Burke · Gang Yao · Dongsheng Duan · Michael A. Rudnicki

Received: 14 September 2026 / Accepted: 12 November 2026
© The Author(s) 2026

Abstract

Background Duchenne muscular dystrophy (DMD) is an X-linked recessive disorder caused by the loss of functional dystrophin protein, resulting in progressive muscle degeneration in skeletal muscle due to myofiber fragility and muscle stem cell dysfunction. Satellos Biosciences developed an orally available small molecule SAT-3247 to promote repair and regeneration of injured skeletal muscle. SAT-3247 inhibits the kinase AAK1 to increase membrane localization of NUMB, resulting in enhanced polarity, increased numbers of asymmetric divisions, and increased generation of progenitors. Therefore, a pilot study was conducted with a mixed breed DMD canine model to explore the potential for SAT-3247 treatment to impact repair and regeneration of injured skeletal muscle.

Case presentation Two 9-month-old DMD dogs were treated for a period of 18 weeks, with oral delivery of SAT-3247 for 4 consecutive days per week (i.e., 3 days off) at 10 mg/kg dose. SAT-3247 treatment resulted in improved muscle morphology, decreased infiltration of inflammatory cells, increased regenerative index (measuring the ratio of regenerating to necrosing cells) in multiple muscles, improvement in locomotory parameters in both forelimb and hindlimbs including greater force generation with no cardiac toxicity.

Conclusions Overall, this proof-of-concept pilot study in a canine model highlights the therapeutic potential of SAT-3247 to repair and regenerate injured muscle and serve as a treatment for DMD. Together, these data provide a compelling preclinical groundwork for advancing SAT-3247 towards clinical evaluation in DMD patients.

Keywords Duchenne muscular dystrophy (DMD) · Dystrophin · Canine DMD model · SAT-3247 · Regenerative Index (RI) · Regenerating myofibers · Necrotic myofibers · Tetanic force · Torque Force · Cardiac function

This Article in Press is shared early to give you faster access to new research. It is citable and carries a permanent DOI. The final edited version will replace it automatically.

https://doi.org/10.1186/s13395-026-00463-0

Published online: 17 November 2026

Background

Duchenne muscular dystrophy (DMD) is an X-linked degenerative muscle disease with a prevalence of 4.8 in 100,000 males worldwide [1, 2]. The *DMD* gene is the largest known human gene with 79 exons spanning 2.2 Mb [1]. Loss-of-function mutations in the *DMD* gene result in the loss of functional dystrophin. Clinical delays in motor-milestones in DMD patients become notable between 2 and 5 years of age. Disease progression occurs rapidly, resulting in many patients becoming wheelchair-bound by 12 years of age. Typically, respiratory failure due to skeletal muscle weakness together with heart failure result in death in the second or third decade of life [3].

Dystrophin is a component of the large oligomeric dystrophin-glycoprotein complex (DGC) that spans the sarcolemma of myofibers in skeletal and cardiac muscle [4]. The DGC acts to connect the actin/microtubule cytoskeleton of the myofiber to the surrounding extracellular matrix. Lack of functional dystrophin impairs DGC assembly making muscle prone to injury. In skeletal muscle, constant cycles of degeneration together with impaired regeneration lead to increasing levels of inflammation and fibrosis, progressive muscle weakening and loss of motor function [5].

Dystrophin is highly expressed in activated muscle stem cells where it localizes to the basal cortex and recruits the kinase Mark2, an important regulator of cell polarity. In the absence of dystrophin, cell polarity fails to be properly established, a component of the PAR-complex called Pard3 is no longer localized to the apical cortex, and the number of asymmetric divisions is significantly reduced [6, 7]. Many of these cells develop abnormal numbers of centrosomes, leading to mitotic arrest [7, 8]. Moreover, the loss of polarity establishment in dystrophin-deficient muscle stem cells results in altered epigenetic control of gene expression due to reduced nuclear translocation of the arginine methyltransferase Carm1 [9]. Consequently, the reduced generation of progenitors together with arrested cells results in impaired regeneration in adult skeletal muscle [10, 11] and impaired secondary myogenesis during fetal development [11] in *mdx* mice.

The current standard of care, corticosteroids, along with gene-targeting and exon skipping therapies, and other small molecule approaches for DMD may prolong ambulation and improve survival into adulthood. However, the disease remains relentlessly progressive, and most continue to experience life-limiting respiratory and/or cardiac complications preventing a normal lifespan [12, 13]. Taken together, there is an urgent need for more effective and widely accessible treatments for DMD.

Satellos Bioscience developed SAT-3247, an orally available small molecule drug intended to treat DMD by promoting repair and regeneration of injured skeletal muscle. SAT-3247 restores polarity of satellite cells by inhibiting AAK1, a kinase that phosphorylates NUMB, resulting in its removal from the membrane. Notably, AAK1 deletion restores NUMB polarization and asymmetric division of DMD muscle stem cells [11]. The therapeutic efficacy and safety profile of SAT-3247 are currently under Phase 2 clinical investigation in both pediatric [14] and adult cohorts of DMD patients [15]. A phase 1 study [16] evaluated the safety and tolerability of SAT-3247 in healthy volunteers and adult DMD participants. In addition, over the 28-day evaluation period, DMD adult participants showed encouraging improvements in muscle strength. While active phase 2 clinical trials are now underway to assess the therapeutic efficacy of SAT-3247, this article will present the preclinical data in an outbred DMD canine model [17] where SAT-3247 was administered for a period of 18 weeks. Multiple parameters were evaluated including body weights, histological endpoints, motor and cardiac function functional assessments, and clinical pathology parameters.

Table 1 Details of DMD dogs

	Study DMD-1	Study DMD-2
Sex	Male	Female
Body Weight at Initiation of Dosing	9.07 kg	13.61 kg
Genotype	Homozygous	
Date of birth	23 Feb 2023	
Age at Initiation of Dosing	8.9 months old	
Initiation of Dosing	14 Nov 2023	
Completion of the study	19 Mar 2024	
Strain/Breed	Mixed breed DMD canine model comprising golden retriever, Labrador retriever, beagle and Welsh corgi breeds with intronic insertion in intron 19 of DMD	

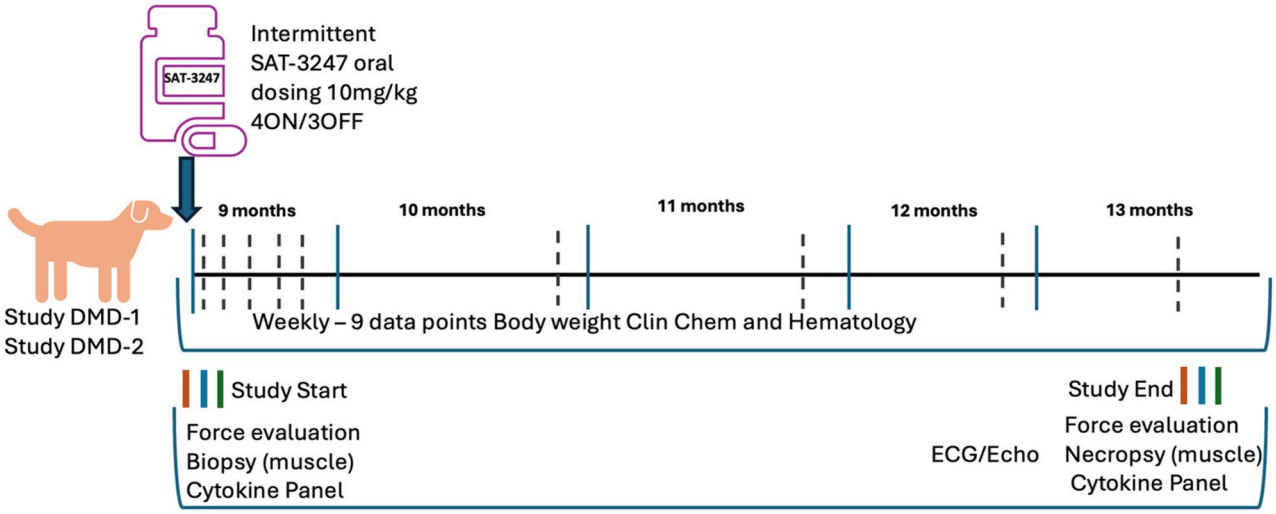

Fig. 1 Schematic representation of the dosing schedule, sample collection. SAT-3247 dosing strategy with sample acquisition timelines are depicted. Body weight and diagnostic assessment measurements were taken on weekly basis. Samples for cytokine profiling collected before the start of the study and end of the study. For muscle regeneration assessments, biopsies were collected before the start of the study and necropsies were collected at the end of the study. Muscles collected include *biceps femoris*, *vastus lateralis*, *diaphragm*, *gastrocnemius medial* and *gastrocnemius lateral*. Force measurements were also performed before and after dosing SAT-3247

Case presentation

Dog history

To better reflect the phenotypic heterogeneity of human DMD, the mixed breed canine DMD model comprising golden retriever, Labrador retriever, beagle and Welsh corgi breeds was used. Affected dogs carry the LRMD mutation in DMD, an intronic insertion in intron 19 [17, 18]. The DMD dogs exhibit a progressive and ultimately fatal course of disease [19]. The progression of the disease in dogs closely mimics human patients, showing variable fiber size, fat accumulation, macrophage infiltration, central nucleation and fibrosis. Two 9-month-old DMD dogs (*Study DMD-1* and *Study DMD-2*) were used in this pilot study (Table 1). Schematic representation of the dosing schedule and sample collection is shown in Fig. 1. DMD dogs were dosed with SAT-3247 (10 mg/kg PO) for 18 weeks with 4 days on and 3 days off schedule. Intermittent drug treatment was undertaken to facilitate the cyclic nature of muscle regeneration [20]. In parallel, age-matched normal and dystrophic dogs/samples were evaluated where possible. Researchers were blinded to treatment status for histological analysis.

Pharmacokinetic studies were conducted in beagle dogs receiving SAT-3247 orally once a day for 11 days demonstrated rapid absorption with a peak at 0.5 hand a stable elimination every 4 h with > 99% of the drug eliminated by 24 h (Supplemental Fig. 1a). The rapid clearance and clean 24 h kinetic profile has been fully validated by the IV reference group. This confirms that drug is not accumulated. Further, samples analyzed from *Study DMD-1* and *Study DMD-2* dosed at 10 mg/kg for 16 weeks is shown in Supplemental Fig. 1b.

Body weights

Individual body weights of *Study DMD-1* and *Study DMD-2* were measured one week prior to dose initiation, then weekly during the treatment period to assess treatment-related body weight effects. Additionally, as part of the routine schedule at the testing site, body weights were collected for both dogs starting from the age of 6.2 months (Supplemental Table 1).

Study DMD-1 weighed 9.1 kg and *Study DMD-2* weighed 12.7 kg at 6.2 months of age. Before dosing, at 8.9 months of age *Study DMD-1* was 9.07 kg and *Study DMD-2* was 13.61 kg. From the age of 8.9 months to the completion of dosing at 13.0 months of age there was no loss of body weight indicating that SAT-3247 did not have any negative effects on the overall body weight of the experimental dogs tested. Conversely, both dogs had a 1.2-fold increase in body weight from dose initiation through to the end of the study at 13 months of age.

Histological analyses

All the muscle samples were received either in the form of OCT block or slides with sectioned muscle (10 µm thick). The muscles that were received as tissue blocks were cryostat sectioned (10 µm). For *biceps femoris* muscles, biopsies were collected immediately pre-treatment for *Study DMD-1* and *Study DMD-2* dogs. At necropsy, following 4-months of treatment with SAT-3247, tissue samples were collected from the *biceps femoris*, *diaphragm*, *vastus lateralis*, *gastrocnemius lateral* and *gastrocnemius medial* muscles of the DMD dogs. Tissue samples were also collected from untreated DMD dogs as concurrent controls. For pre-treatment biopsy samples (start), five independent needle biopsies were performed. Biopsy and necropsy samples were snap-frozen in OCT embedding media by submersion in liquid nitrogen-cooled 2-methylbutane. Three biopsies were sectioned (10 µm) whereas necropsy samples were sectioned (10 µm) at three levels separated by a minimum of 100 µm thus providing three technical replicates.

Pre-treatment and post-treatment *biceps femoris* samples, and untreated and treated *diaphragm*, *vastus lateralis*, *gastrocnemius lateral* and *gastrocnemius medial* samples were assessed by immunostaining. Muscle sections were incubated with primary antibodies Rabbit Anti-Laminin (Sigma L9393, Dilution − 1:1000), Goat anti-dog IgG (Abcam AB112849, Dilution − 1:200) and Mouse anti-eMHC IgG1 mAb (Santa Cruz sc-53091, Dilution − 1:200) for 1 h at RT followed by washes with PBS thrice, and incubated with species specific secondary antibodies for 30 min at RT. After incubation slides were washed thrice with PBS before adding DAPI for 5 min to visualize the nuclei. All slides were scanned on a Zeiss Axio Observer Z1/7 microscope. Image sizes were generally restricted to 7 × 7 fields of view, resulting in 49 tiles stitched together into a single large image for quantification.

Following the laminin trace as described in our previous study [21] minimum Feret's diameters of myofibers were determined. Healthy dogs exhibit a uniform, resting architecture with a mean minimum feret of 26.8 µm. Untreated DMD dogs exhibit enlarged myofibers with a mean of minimum feret of 35 µm (Fig. 2). Accordingly, prior to the start of SAT-3247 treatment at 9 months of age *Study DMD-1* and *Study DMD-2* exhibited an elevated mean minimum feret of more than 30 µm (Supplemental Fig. 2a). SAT-3247 treatment mitigated this structural expansion, yielding respective reductions of 15% and 9% in mean minimum feret in *Study DMD-1* (blue) and *Study DMD-2* (red) after treatment (Fig. 2), as well as reductions compared to untreated DMD controls.

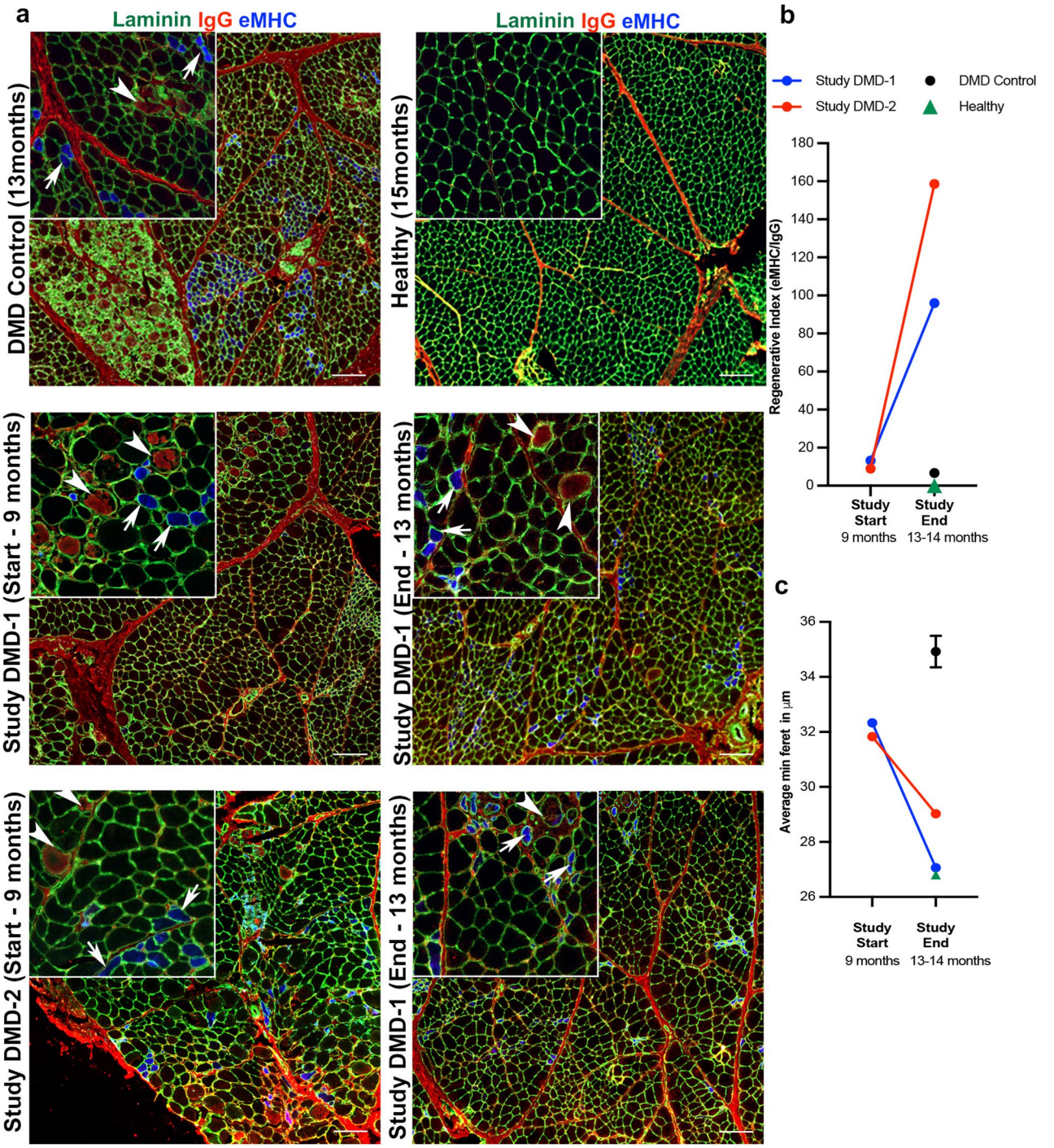

Fig. 2 SAT-3247 treatment enhances increased Regenerative Index (RI) and decreased minimal fiber feret. **a** Representative immunofluorescence image of *biceps femoris* muscle sections of DMD (untreated), healthy, *Study DMD*-1 and *Study DMD*-2 stained for IgG (red, indicated with arrowheads) and embryonic myosin heavy chain (eMHC, blue, indicated with arrows) **b** Graph shows the regenerative index of all the four sample groups. *Study DMD-1* (blue) and *Study DMD-2* (red) are higher at the end of the study compared to pretreatment with a fold change of 6 and 10, respectively, untreated DMD dogs ($n=4$) healthy dog. **c** Average minimum feret is plotted for all 4 groups. *Study DMD-1*(blue) and *Study DMD-2* (red) show reduction in minimum feret, respectively after treatment with SAT-3247. Scale bar is 200 µm. Error bars represent SEM

https://doi.org/10.1186/s13395-026-00463-0

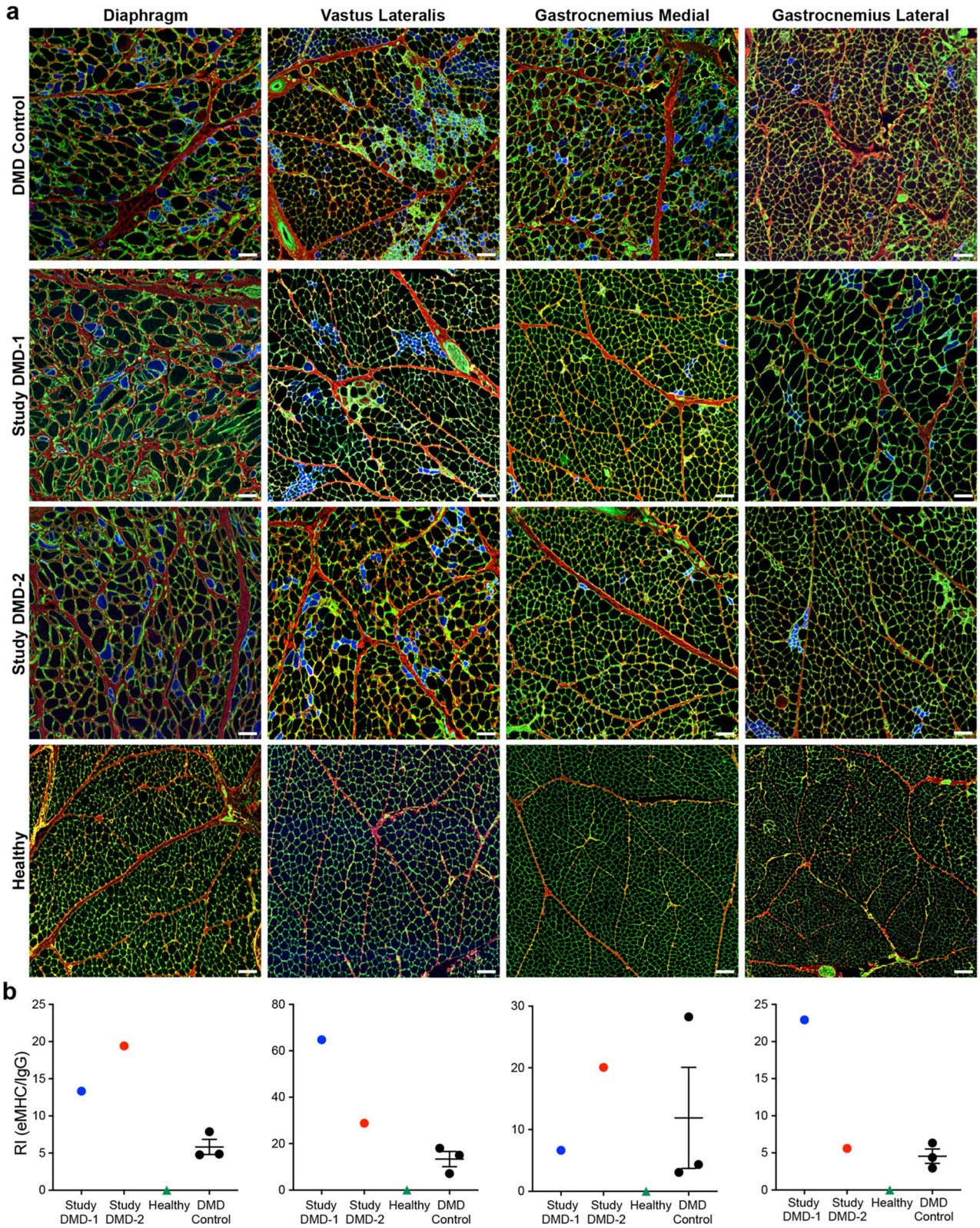

Fig. 3 RI measured for d*iaphragm*, *vastus lateralis*, *gastrocnemius lateral* and *gastrocnemius medial*. **a** Representative immunofluorescence image of four different necropsy muscles stained for IgG (red) and embryonic myosin heavy chain (eMHC, blue) and Laminin (green) of DMD (untreated), healthy, *Study DMD*-1 and *Study DMD*-2 **b** Graphs show the regenerative index of all the four sample groups. In both *diaphragm* and *vastus lateralis* muscles RI in *Study DMD-1* (blue) and *Study DMD-2* (red) is higher compared to untreated DMD controls ($n=3$) with zero RI for healthy dog. Scale bar is 200 µm. Error bars represent SEM

Regenerative Index

Muscle regeneration was assessed using the previously described Regenerative Index (RI) [21]. The components of the RI were measured using Laminin, IgG and eMHC staining in *biceps femoris* (BF) muscles. No signal was observed in secondary only control (Supplemental Fig. 3). To evaluate regenerative activity, newly formed myofibers were identified by immunostaining for expression of embryonic myosin heavy chain (eMHC). Necrotic myofibers were enumerated by immunofluorescent detection of immunoglobulin G (IgG) infiltration (Supplemental Fig. 4 and Supplemental Table 2). The RI was then calculated as the ratio of regenerating ($eMHC^+$) myofibers to necrotic (IgG^+) myofibers.

Strikingly, following 4 months of SAT-3247 treatment of *Study DMD-1* and *Study DMD-2*, RIs were markedly elevated with values of 95.98 and 158.64, respectively, compared to 13.23 and 9.03 RI at the start of the study (Fig. 2b). Untreated DMD dogs ($n=4$) showed a mean RI of 6.64. In healthy dogs, no eMHC fibers were observed (as expected given their skeletal muscles were not injured) with only 0.03% of fibers being IgG positive (also as expected for the same reason); thus, RI is negligible (Supplemental Fig. 2b-c).

When compared to age-matched untreated DMD dogs, other muscles also exhibited a similarly increased RIs following SAT-3247 treatment, including the *diaphragm* and the *vastus lateralis* (Fig. 3a). Magnified images with split channels for IgG and eMHC with Laminin for *diaphragm* and the *vastus lateralis* are shown in Supplemental Fig. 5; and enumerated IgG + and eMHC+ fibers are shown in Supplemental Table 3. The RIs of the *diaphragm* of treated *Study DMD-1* and *Study DMD-2* were both higher with values of 13.34 and 19.42, respectively, compared to a mean of 5.85 in untreated DMD dogs ($n = 3$) (Fig. 3b). The RIs of the *vastus lateralis* of treated *Study DMD-1* and *Study DMD-2* were higher with a value of 64.79 and 28.84, respectively compared to 13.39 RI in untreated DMD dogs ($n = 3$) (Fig. 3b). The RIs of the *gastrocnemius lateral* of treated *Study DMD-1* was higher at 22.93 and was 5.60 for *Study DMD-2* compared to a mean RI of 4.56 RI in untreated DMD ($n = 3$) (Fig. 3b). The RIs of the *gastrocnemius medial* of treated *Study DMD-1* and *Study DMD-2* were 6.65 and 20.07, respectively. Untreated DMD dogs have shown variable results for the *gastrocnemius medial* with a mean of 16.49 ($n = 3$) (Fig. 3b and Supplemental Table 3). Magnified images with split channels for IgG and eMHC with Laminin for *gastrocnemius lateral* and *gastrocnemius medial* are shown in Supplemental Fig. 6; and enumerated IgG + and eMHC+ fibers are shown in Supplemental Table 3. Variable RI in untreated DMD may occur because the *gastrocnemius* group of muscles consistently reveal severe structural degeneration due to extreme compensatory load on ankle extensor [22].

Interestingly, in the *diaphragm* the proportion of myofibers exhibiting IgG infiltration is higher with 4.40% of total fibers IgG^+ in untreated dogs; these levels declined in the SAT-3247 treated dogs to 1% and 0.65% of myofibers in the *diaphragm* being IgG^+. The proportion of $eMHC^+$ myofibers were variable in the *diaphragm* of untreated DMD dogs with a mean of 25.93%. By contrast, 13.40% and 12.67% of myofibers were $eMHC^+$ in post-treatment *Study DMD-1* and *Study DMD-2 diaphragms*, respectively. This suggests that the increase in RI is primarily due to a reduction in necrotic myofibers. However, it is possible that differences in physical activity could contribute to differences in IgG infiltration observed between all of the dogs.

Inflammatory response

To assess the baseline inflammatory response, CD45, a pan-leukocyte marker staining was performed on *biceps femoris* (BF) muscles using Rat anti-dog CD45 (Biorad YKIX716.13, Dilution 1:100) along with Rabbit Anti-Laminin (Sigma L9393, Dilution − 1:1000). Slides were incubated for 1 h followed by washes and incubation with secondary antibodies. No signal was observed in secondary only control (Supplemental Fig. 7). Strikingly, following SAT-3247 treatment of *Study DMD-1* and *Study DMD-2*, the number of $CD45^+$ cells exhibited an approximate 4-fold and 2.5-fold drop, respectively (Fig. 4a and b). The pre-treatment number of $CD45^+$ cells in *Study DMD-1* and *Study DMD-2* were 91 and 72 cells per mm^2, respectively, whereas post-treatment were 23 and 29 cells per mm^2, respectively. Untreated DMD dogs showed a mean of 61.5 ($n = 4$ dogs). In healthy dogs, only 4 $CD45^+$ cells per mm^2 were observed (Fig. 4b). This is in line with the literature which indicates that less than 1–2% $CD45^+$ cells are observed in healthy dogs, increasing 10–15% in DMD [23]. However, the mechanistic basis for the reduction in CD45 + cells will require additional study.

Whole limb function

The contractile force of the flexor and extensor muscle groups was assessed as previously described [24]. Twitch and Tetanic torque were measured for both the forelimbs and hindlimbs of *Study DMD-1* and *Study DMD-2* at the start of the study at 9 months of age (baseline) and after 4 months of treatment at 13 months of age, and expressed as N-cm/kg (Newton-centimeters per kilogram) to measure turning effect (torque) produced by a force applied at a distance and normalized to body weight (Fig. 5), whereas the corresponding contraction force was expressed as N/kg (Newtons per kilogram) to represent force normalized to body weight (Supplemental Fig. 8).

Prior to treatment, *Study DMD-1* and *Study DMD-2* exhibited reduced twitch and tetanic forces for forelimb flexion, hindlimb extension and hindlimb flexion, which is typical of DMD dogs [25]. Following treatment with SAT-3247, *Study DMD-1* and *Study DMD-2* exhibited substantial increase of 51% and 39.3% respectively, in forelimb flexion tetanic force which is higher than untreated dogs of the same colony (Supplemental Fig. 8a).

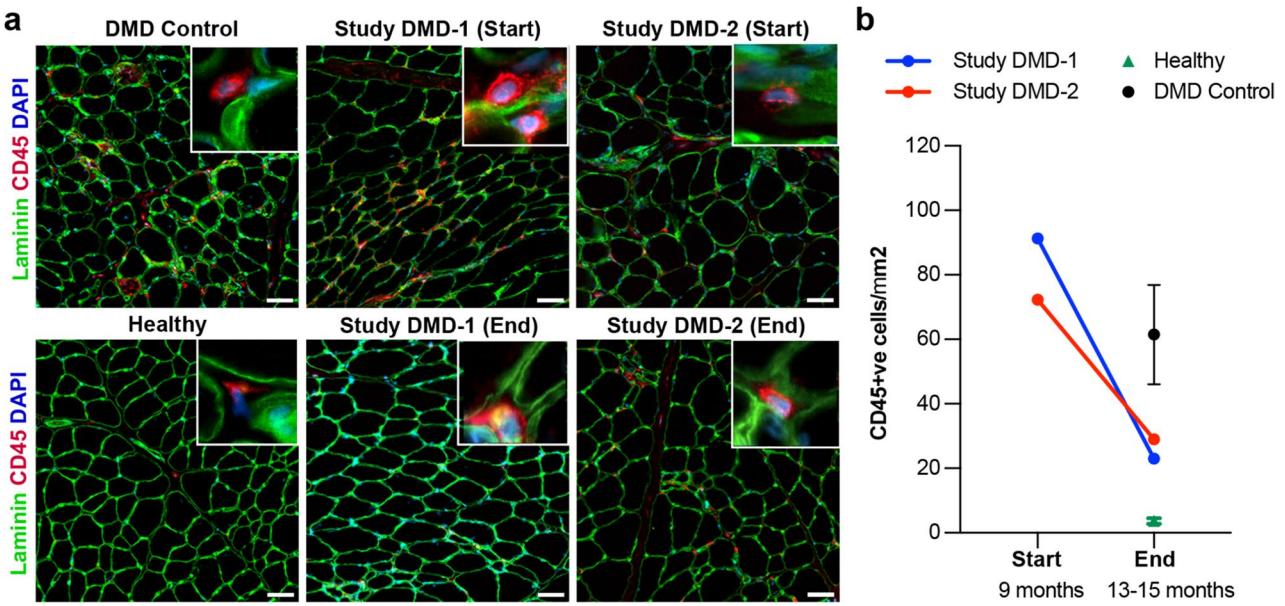

Fig. 4 Marked reduction in leukocyte infiltration in SAT-3247 treated canine muscle. **a** Representative immunofluorescent cross-sections of *biceps femoris* muscle stained for CD45 shown in red, Laminin in green and counterstained with DAPI in blue. **b** $CD45^+$cells were markedly reduced with SAT-3247 treatment. Scale bar is 50 µm. Inserts show magnified image of 28 µm x 28 µm. Error bars represent SEM

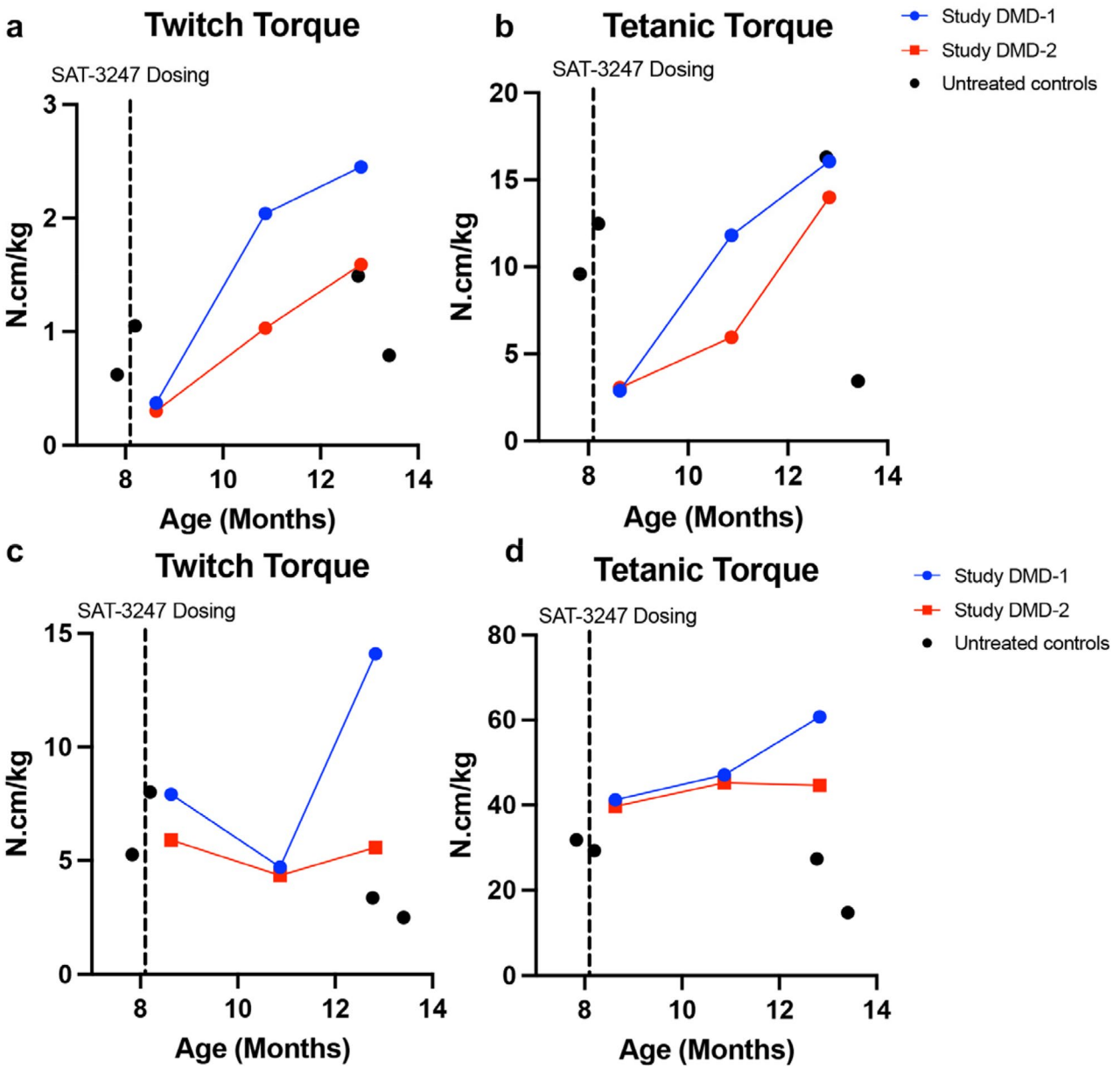

Fig. 5 Whole-limb functional assessment. Hindlimb flexion twitch torque (**a**) and tetanic torque (**b**) increased in *Study DMD-1* (blue) and *Study DMD-2* (red) after dosing with SAT-3247 indicating an increase in muscle function after SAT-3247 treatment. Hindlimb extension twitch torque (**c**) and tetanic torque (**d**) increased in *Study DMD-1* (blue) and *Study DMD-2* (red) after dosing with SAT-3247 indicating an increase in muscle function in *Study DMD-1* and maintained in *Study DMD-2* after SAT-3247 treatment. Independent age-matched untreated dogs (black dots)

Consistently, a 57.5% and 39.9% increase in torque were also observed for *Study DMD-1* and *Study DMD-2*, respectively. Forelimb flexion twitch force exhibited a slight increase in *Study DMD-1* and greater increase of 41.7% in *Study DMD-2* (Supplemental Fig. 8a).

Following treatment with SAT-3247 between 9 months and 13 months of age, hindlimb flexion tetanic torque also increased substantially in *Study DMD-1* and *Study DMD-2* from 2.89 to 16.05 N·cm/kg (+455%) and from 3.06 to 13.99 N·cm/kg (+357%), respectively (Fig. 5). Similarly, hindlimb flexion tetanic force also increased from 0.21 to 1.19 N/kg (+467%) and from 0.20 to 0.93 N/kg (+365%) (Supplemental Fig. 8b). Hindlimb extension of *Study DMD-1* showed marked increases in normalized twitch force (0.57 to 1.05 N/kg, +84%) and tetanic

torque (41.25 to 60.76 N·cm/kg, +47%) between 9 and 13 months of age and in comparison, to untreated dog of same age, indicating preserved or improving muscle function (Fig. 5). *Study DMD-2* demonstrated stable twitch force (0.39 to 0.37 N/kg) and modest increases in tetanic parameters, suggesting partial maintenance of strength, perhaps due to sex differences.

Spatiotemporal gait analysis

To evaluate functional locomotion, spatiotemporal parameters of canine gait were assessed focusing on stride length and stride velocity (Supplemental Fig. 9). Stride length was measured for both *Study DMD-1* and *Study DMD-2* from 6.2 to 12.8 months of age. Following treatment with SAT-3247, there was an increase of stride length of at least 7 cm in *Study DMD-1* and 13 cm in *Study DMD-2*. At the end of the treatment period at 13 months of age *Study DMD-1* had an average stride length of 74 ± 5.7 cm and *Study DMD-2* had an average stride length of 77 ± 5.9 cm (Supplemental Fig. 9a). Both *Study DMD-1 and Study DMD-2* displayed highly consistent stride lengths, with less than 0.5% bilateral variance across both forelimb and hindlimb pairs. From baseline to 9.83 months of age, velocity was increased from 108.4 cm/s to 125.0 cm/s in *Study DMD-1* and from 93.5 cm/s to 136 cm/s in *Study DMD-2* (Supplemental Fig. 9b). Velocity was maintained above 100 cm/s thereafter with a slight drop for *Study DMD-2* at 10.79 months. At the end of the study at 13 months of age, average velocity of *Study DMD-1* was 120 ± 13 cm/s and *Study DMD-2* was 112 ± 14 cm/s.

Cardiac function

To assess the heart function, an echocardiogram was performed for both *Study DMD-1* and *Study DMD-2* upon completion of treatment. All of the data collected and analyzed is based on the standard protocols documented in [24]. Left ventricular ejection fraction (LVEF), which is the percentage of blood pumped out of the left ventricle with each heartbeat, was reported as 57.2% and 63.2% for *Study DMD-1* and *Study DMD-2*, respectively (Supplemental Table 4). Fractional shortening (FS), a measure of left ventricular systolic function, was found to be 37.70% and 30.63% in *Study DMD-1* and *Study DMD-2*, respectively. As reported in the literature, DMD dogs at 13 months of age, typically exhibit an LVEF of 43.3±3.7 and a FS of 24.7±0.9% [26]. Untreated dogs of the same colony show similar readings (Supplemental Table 4) indicating lack of cardiac toxicity. Heart rate was 120 bpm for *Study DMD-1* and 160 bpm for *Study DMD-2.* Other parameters such as P wave and PR interval, QRS complex, QT interval and ST segment values were within the range of a normal dog with no signs of prolonged conduction interval (P-R, QRS, QT) changes that are usually detectable in DMD dogs at this age [27].

Serological analysis

Clinical Pathology (hematology and clinical chemistry) procedures were undertaken at the University of Missouri Veterinary Diagnostic Laboratory. During the period of the study, there were no alterations in platelet count, liver function (GLDH), and kidney function (BUN) (Supplementary Fig. 10a-c). Other hematology and blood biochemistry biomarkers were also unremarkable. Creatine kinase (CK) levels were slightly reduced at 13 months following SAT-3247 treatment in *Study DMD-1* from 13,015 U/L to 11,430 and a substantial drop in *Study DMD-2*, female dog from 38,621 to 9,646 (~ 75%) (Supplemental Fig. 10d). Both the endpoint CK levels in treated dogs were lower in comparison to the age-matched untreated dogs with 39,908 U/L (Supplementary Fig. 10e). However, CK remained elevated in both the dogs (> 9000 U/L) compared to normal controls (< 200 U/L), indicating ongoing muscle damage [28].

Serum cytokines were quantified by multiplex Luminex cytokine detection assay according to our published protocol [29]. The concentration of various cytokines, including GM-CSF, IFN-g, IL-2, IL-6, IL-7, IL-8, IL-15, IP-10, KC-Like, IL-10, IL-18 and MCP-1 (CCL2) were determined to assess SAT-3247 activity on immunomodulation in *Study DMD-1* and *Study DMD-2*. Following treatment of *Study DMD-1*, male dog with SAT-3247,

a marked immunomodulatory response was observed, characterized by substantial increases in the anti-inflammatory cytokine IL-10 (15-fold) alongside significant reductions in pro-inflammatory mediators such as GM-CSF, IL-2, IL-6, IL-7, and IL-18 (Supplemental Fig. 11a and 11b), with IFN-γ remaining elevated. However, in *Study DMD-2*, levels of GM-CSF, IL-2, IL-6, IL-7, and IL-18 were reduced, other cytokine levels largely trended toward baseline, with IFN-γ remaining elevated but less dramatically, and no change in IL-10. Additionally, pro-inflammatory cytokine IL-18, showed consistent suppression in both dogs with a fold change of 0.29 and 0.48 in *Study DMD-1* and *Study DMD-2*, respectively. CCL2 levels before dosing were 463.34 pg/mL and 1,289.43 pg/mL in *Study DMD-1* and *Study DMD-2*, respectively. At the end of the study, the CCL2 levels were 471.81 pg/mL and 637.76 pg/mL in *Study DMD-1* and *Study DMD-2*, respectively. The CCL2 level did not change appreciably in *Study DMD-1* but decreased in *Study DMD-2*.

Discussion

Prolonged SAT-3247 treatment in DMD dogs appears safe, well-tolerated, and the phenotypic analysis is suggestive of therapeutic activity. Both DMD dogs dosed with SAT-3247 for 18 weeks exhibited substantial histological and kinetic profile, as evidenced by increased RI and increased muscle force generation. These findings in the treated DMD dogs are in contrast with the typical muscle and force generation observed in DMD-affected models at a similar age, where active regeneration markers decline with progressive and extensive fibrotic remodeling, and a marked decline in force generation [30, 31]. Morphometric assessment of myofibers of the *biceps femoris* muscle revealed a downward shift in minimum feret of myofibers in SAT-3247 treated DMD dogs suggesting a normalization of the muscle tissue due to potential therapeutic efficacy of the intervention.

Determination of RI was developed as a method to assess regeneration potential specifically for DMD [21]. The RI is the ratio of newly formed ($eMHC^+$) myofibers to necrotic (IgG^+) myofibers, thus normalizing the variation found between samples and between sections. Accordingly, the RI integrates both regenerative and degenerative states to assess the net regenerative potential of muscle. Importantly, RI was found to significantly decline by about 2.5-fold in paediatric DMD patients between 7 and 11 years of age [21]. Notably, after treatment with SAT-3247 a substantial increase in RI was observed in *biceps femoris*, *diaphragm*, and *vastus lateralis*. High variability among untreated DMD dogs of the *gastrocnemius lateral* and *gastrocnemius medial* muscle makes comparisons problematic. Overall, in untreated 13-month-old DMD dogs, the average RI value was approximately 6.6. Notably, following 18-weeks of SAT-3247 treatment in DMD dogs, RIs were 95.98 and 158.64 for the two treated animals with increases between 7.25-fold to 17.57-fold from baseline to the end of dosing. These data suggest that SAT-3247 is constructively impacting the repair and regeneration of injured skeletal muscle and supports the potential utility of RI determination as a method to assess the regenerative potential of candidate therapies.

Importantly, muscle force and torque of SAT-3247-treated dogs also showed marked increases between 9 and 13 months of age, contrasting with the progressive decline typically observed in DMD dogs. For example, forelimb flexion tetanic force and torque increased substantially by 40–50%. Hindlimb flexion tetanic force and torque showed dramatic increases of > 300%. Hindlimb extension twitch/tetanic force and torque increased up to 84%. Thus SAT-3247-treated DMD dogs did not appear to exhibit the declines in force generation typically observed in DMD dogs, and were capable of generating force approaching that of healthy dogs [25, 32].

Determination of LVEF and FS represent the primary hallmarks to measure onset and progression of DMD-associated cardiomyopathy. In canine DMD, cardiac function remains stable for the first 6 months; followed by a pronounced decline in LVEF and FS thereafter and the development of dilated cardiomyopathy after 30 months [27, 33]. A decrease in FS below 27% is a critical clinical cutoff below which indicates transition from compensation to systolic dysfunction [33, 34], while healthy dogs maintain an FS of 30–45%. Notably, following SAT-3247 treatment, there was no observed marked decline in cardiac function. Instead, both LVEF and FS remained within the normal range. These data suggest that SAT-3247 is not detrimental to cardiac function. Further studies are

required to determine whether SAT-3247 may provide cardioprotective benefits and to understand the potential mechanism of action.

Another hallmark of DMD is chronic, muscle-wide inflammation wherein a massive immune response recruits inflammatory cells and loads the muscle tissue with a distinct profile of cytokines and chemokines [35]. In the absence of dystrophin, DGC assembly is impaired which renders muscle fibers susceptible to injury. Constant contraction-induced stress results in continuous cycles of degeneration and regeneration. Subsequent accumulation of inflammation contributes to progressive muscle weakening [36]. Thus, the chronic inflammatory environment plus intrinsic dystrophin-related defects of satellite cells makes them less effective at producing functional new muscle [37].

Cytokine profiling revealed an increase in anti-inflammatory cytokines IL-10 (15-fold) *in Study DMD-1* coupled with decreases in pro-inflammatory cytokines including GM-CSF, IL-2, IL-6, IL-7, and IL-18 in both *Study DMD-1* and *Study DMD-2*. This suggests a shift toward a more regenerative immune environment, contrasting with the heightened inflammation typically seen in DMD dogs, in alignment with observations made in *mdx* mice and human tissues [38]. IL-10 forces transition of M1 to M2 macrophages [39] and is considered to act as a double-edged sword, as at later stages of DMD it may over-activate fibro-adipogenic progenitors (FAPs). Interestingly, the number of $CD45^{+}$ cells decreased with SAT-3247 treatment potentially as a consequence of enhanced muscle regeneration. Further studies will be required to better understand the effects long-term treatment with SAT-3247 has on inflammation.

Creatine kinase (CK) levels remained elevated as untreated DMD compared to normal controls, indicating ongoing muscle damage [28], consistent with the expectation that SAT-3247 treatment does not prevent damage. The ongoing muscle-fiber damage initiates a regenerative response, with satellite cells responding to that damage to repair and regenerate muscle. However, this response may not be sufficient to prevent ongoing muscle injury or reduce CK levels, particularly in the context of persistent dystrophin deficiency and chronic inflammation.

The variation in response between *Study DMD-1* and *Study DMD-2* may reflect sex differences. *Study DMD-1* is a male dog whereas *Study DMD-2* is female. Female DMD dogs generally express a milder clinical disease course [40, 41]. At the molecular level, females show a significant downregulation of calcium-binding transcripts in heart relative to males [42]. Nevertheless, this study has shown an increase or improvement in RI, hindlimb function, length of stride, heart fractional shortening with a reduction in inflammation in both dogs that were tested.

Conclusion

We present a case report of two DMD dogs treated for 18 weeks with SAT-3247, an investigational new drug designed to promote polarity and restore muscle stem cell function by promoting asymmetric cell divisions, thus stimulating regeneration. Results are consistent with the proposed mechanism of action and support the assertion that SAT-3247 enhances skeletal muscle regeneration. The treated DMD dogs show an overall improvement in force measurements, increased RI, improved muscle architecture, and possess a cytokine profile consistent with decreased inflammation. However, a limitation of this study is that no statistical analysis can be performed due to the small number of dogs available for drug testing together with an absence of a placebo control group. Nevertheless, this proof-of-concept pilot study in a canine DMD model highlights the therapeutic potential of SAT-3247 as a treatment for DMD. Together, these data provide a compelling preclinical groundwork for advancing SAT-3247 towards clinical evaluation in DMD patients.

Abbreviations

AAK-1 Adapter-associated kinase-1
BUN Blood urea nitrogen

CD45	Cluster of differentiation
DMD	Duchenne Muscular Dystrophy
eMHC	Embryonic Myosin Heavy Chain
FS	Fractional shortening
GLDH	Glutamate dehydrogenase
IgG	Immunoglobulin G
LVEF	Left ventricular ejection fraction
MFF	Minimal fiber Feret (minimal Feret's diameter)
PBS	phosphate-buffered saline
RI	Regenerative Index
RT	Room temperature
DAPI	4′,6-diamidino-2-phenylindole

Supplementary Information The online version contains supplementary material available at https://doi.org/10.1186/s13395-026-00463-0.

Acknowledgements The authors thank the University of Ottawa Imaging Core for use of microscopes and training required for scanning of entire muscle biopsy sections. We also thank Jin Han, Keqing Zhang and Charis McPherson for expert technical assistance. We extend our thanks to Dr. Wildon Farewell for careful reading of the manuscript.

Authors' contributions SSSR, JKS, PL, RM, TM, GY, DD, FG and MAR made contributions to the conception, data analysis and analyzed data. JJ designed and developed the drug. SSSR wrote the paper. JAT, YY, MJB, GY, JGM performed experiments. MAR, SSSR, PL, RM, TM and JKS designed the experiments and edited the manuscript.

Funding This study was supported by research contracts from Satellos Bioscience to DD and MAR. The data from untreated control dogs were generated with the support of NIH grants NS90634 and NS131416 to DD.

Data availability All data needed to evaluate the conclusions in the paper are present in the paper. Any additional information required to reanalyze the data reported in this work paper is available from the lead contact (mrudnicki@ohri.ca).

Declarations

Ethics approval and consent to participate All animal experiments were conducted at the University of Missouri and approved by the Animal Care and Use Committee of the University of Missouri, as per all relevant ethical regulations for animal testing.

Competing interests MAR is the Founding Scientist and Chief Discovery Officer of Satellos Bioscience and receives consulting remuneration and holds stocks and options. SSSR, JKS, PL, JJ, TM, RM and FG are employees of Satellos Bioscience and hold stock and/or options. The remaining authors declare no conflict of interest.

Open Access This article is licensed under a Creative Commons Attribution-NonCommercial-NoDerivatives 4.0 International License, which permits any non-commercial use, sharing, distribution and reproduction in any medium or format, as long as you give appropriate credit to the original author(s) and the source, provide a link to the Creative Commons licence, and indicate if you modified the licensed material. You do not have permission under this licence to share adapted material derived from this article or parts of it. The images or other third party material in this article are included in the article's Creative Commons licence, unless indicated otherwise in a credit line to the material. If material is not included in the article's Creative Commons licence and your intended use is not permitted by statutory regulation or exceeds the permitted use, you will need to obtain permission directly from the copyright holder. To view a copy of this licence, visit http://creativecommons.org/licenses/by-nc-nd/4.0/.

References

1. Hoffman EP, Brown RH, Kunkel LM, Dystrophin. The protein product of the duchenne muscular dystrophy locus. Cell. 1987;51(6):919–28. https://doi.org/10.1016/0092-8674(87)90579-4.
2. Duan D, Goemans N, Takeda S, Mercuri E, Aartsma-Rus A. Duchenne muscular dystrophy. Nat Rev Dis Primer. 2021;7(1):13. https://doi.org/10.1038/s41572-021-00248-3.
3. Emery AE. The muscular dystrophies. Lancet. 2002;359(9307):687–95. https://doi.org/10.1016/S0140-6736(02)07815-7.
4. Ervasti JM, Campbell KP. Membrane organization of the dystrophin-glycoprotein complex. Cell. 1991;66(6):1121–31. https://doi.org/10.1016/0092-8674(91)90035-W.
5. Mann CJ, Perdiguero E, Kharraz Y, Aguilar S, Pessina P, Serrano AL, et al. Aberrant repair and fibrosis development in skeletal muscle. Skelet Muscle. 2011;1(1):21. https://doi.org/10.1186/2044-5040-1-21.
6. Le Roux I, Konge J, Le Cam L, Flamant P, Tajbakhsh S. Numb is required to prevent p53-dependent senescence following skeletal muscle injury. Nat Commun. 2015;6(1):8528. https://doi.org/10.1038/ncomms9528.
7. Dumont NA, Wang YX, Rudnicki MA. Intrinsic and extrinsic mechanisms regulating satellite cell function. Development. 2015;142(9):1572–81. https://doi.org/10.1242/dev.114223.
8. Granet JA, Robertson R, Cusmano AA, Filippelli RL, Lorenz TO, Li S, et al. Muscle stem cells in Duchenne muscular dystrophy exhibit molecular impairments and altered cell fate trajectories impacting regenerative capacity. Cell Death Dis. 2025;16(1):437. https://doi.org/10.1038/s41419-025-07755-1.
9. Chang NC, Sincennes MC, Chevalier FP, Brun CE, Lacaria M, Segalés J, et al. The Dystrophin Glycoprotein Complex Regulates the Epigenetic Activation of Muscle Stem Cell Commitment. Cell Stem Cell. 2018;22(5):755–e7686. https://doi.org/10.1016/j.stem.2018.03.022.
10. Chang NC, Chevalier FP, Rudnicki MA. Satellite Cells in Muscular Dystrophy – Lost in Polarity. Trends Mol Med. 2016;22(6):479–96. https://doi.org/10.1016/j.molmed.2016.04.002.
11. Esper ME, Lin AYT, Bennett D, Rudnicki MA. Intrinsic dysfunction in muscle stem cells lacking dystrophin begins during secondary myogenesis. Nat Commun. 2025;16(1):10031. https://doi.org/10.1038/s41467-025-64999-3.
12. Mah JK. Therapeutic options for Duchenne muscular dystrophy: hope or hype? Ther Adv Neurol Disord. 2025;18:17562864251346326. https://doi.org/10.1177/17562864251346326.
13. Lochmüller H, Gonorazky H, Nigro E, Mah JK, Alemán A, Yaworski A, et al. Results of a phase II open-label, multiple-dose study of vamorolone (VBP15-006) in 7- to <18-year-old boys with duchenne muscular dystrophy. J Neurol. 2026;273(3):177. https://doi.org/10.1007/s00415-026-13711-6.
14. NCT07287189 [Internet]. Available from: https://clinicaltrials.gov/study/NCT07287189
15. NCT06867107 [Internet]. Available from: https://clinicaltrials.gov/study/NCT06867107
16. NCT06565208 [Internet]. Available from: https://clinicaltrials.gov/study/NCT06565208
17. Smith BF, Kornegay JN, Duan D. 130. Independent Canine Models of Duchenne Muscular Dystrophy Due to Intronic Insertions of Repetitive DNA. Mol Ther. 2007;15:S51. https://doi.org/10.1016/S1525-0016(16)44336-4.
18. Hakim CH, Kumar SRP, Pérez-López DO, Wasala NB, Zhang D, Yue Y, et al. Cas9-specific immune responses compromise local and systemic AAV CRISPR therapy in multiple dystrophic canine models. Nat Commun. 2021;12(1):6769. https://doi.org/10.1038/s41467-021-26830-7.
19. Teixeira J, Burke MJ, Herzog RW, Duan D. Canine Model of Duchenne Muscular Dystrophy. In: Flanigan K, Nicolau S, editors. Duchenne Muscular Dystrophy [Internet]. New York, NY: Springer US; 2026[cited 2026 Aug 19]. pp. 203–38. (Methods in Molecular Biology). Available from: https://link.springer.com/https://doi.org/10.1007/978-1-0716-4811-7_14doi:10.1007/978-1-0716-4811-7_14.
20. Cutler AA, Pawlikowski B, Wheeler JR, Dalla Betta N, Elston T, O'Rourke R, et al. The regenerating skeletal muscle niche drives satellite cell return to quiescence. iScience. 2022;25(6):104444. https://doi.org/10.1016/j.isci.2022.104444.
21. Smid JK, McPherson CA, Monast JG, Rayagiri SSS, Moore SA, Rudnicki MA. Regenerative Index: a method to assess muscle regeneration in patients with Duchenne muscular dystrophy. Skelet Muscle. 2026;1. https://doi.org/10.1186/s13395-026-00436-3.
22. Kornegay JN, Childers MK, Bogan DJ, Bogan JR, Nghiem P, Wang J, et al. The Paradox of Muscle Hypertrophy in Muscular Dystrophy. Phys Med Rehabil Clin N Am. 2012;23(1):149–72. https://doi.org/10.1016/j.pmr.2011.11.014.
23. Rouger K, Larcher T, Dubreil L, Deschamps JY, Le Guiner C, Jouvion G, et al. Systemic Delivery of Allogenic Muscle Stem Cells Induces Long-Term Muscle Repair and Clinical Efficacy in Duchenne Muscular Dystrophy Dogs. Am J Pathol. 2011;179(5):2501–18. https://doi.org/10.1016/j.ajpath.2011.07.022.
24. Hakim CH, Teixeira J, Leach SB, Duan D. Physiological Assessment of Muscle, Heart, and Whole Body Function in the Canine Model of Duchenne Muscular Dystrophy. In: Maruyama R, Yokota T, editors. Muscular Dystrophy Therapeutics [Internet]. New York, NY: Springer US; 2023[cited 2026 Aug 17]. pp. 67–103. (Methods in Molecular Biology). Available from: https://link.springer.com/https://doi.org/10.1007/978-1-0716-2772-3_5doi:10.1007/978-1-0716-2772-3_5.

25. Kornegay JN, Bogan DJ, Bogan JR, Childers MK, Cundiff DD, Petroski GF, et al. Contraction force generated by tarsal joint flexion and extension in dogs with golden retriever muscular dystrophy. J Neurol Sci. 1999;166(2):115–21. https://doi.org/10.1016/S0022-510X(99)00118-5.
26. Ait Mou Y, Lacampagne A, Irving T, Scheuermann V, Blot S, Ghaleb B, et al. Altered myofilament structure and function in dogs with Duchenne muscular dystrophy cardiomyopathy. J Mol Cell Cardiol. 2018;114:345–53. https://doi.org/10.1016/j.yjmcc.2017.12.008.
27. Barthélémy I, Su JB, Cauchois X, Relaix F, Ghaleb B, Blot S. Ambulatory electrocardiographic longitudinal monitoring in a canine model for Duchenne muscular dystrophy identifies decreased very low frequency power as a hallmark of impaired heart rate variability. Sci Rep. 2024;14(1):8969. https://doi.org/10.1038/s41598-024-59196-z.
28. Kornegay JN, Spurney CF, Nghiem PP, Brinkmeyer-Langford CL, Hoffman EP, Nagaraju K. Pharmacologic Management of Duchenne Muscular Dystrophy: Target Identification and Preclinical Trials. ILAR J. 2014;55(1):119–49. https://doi.org/10.1093/ilar/ilu011.
29. Hakim CH, Kumar SRP, Pérez-López D, Teixeira J, Herzog RW, Duan D. Assessment of the Gene Therapy Immune Response in the Canine Muscular Dystrophy Model. In: Maruyama R, Yokota T, editors. Muscular Dystrophy Therapeutics [Internet]. New York, NY: Springer US; 2023[cited 2026 Sep 7]. pp. 353–75. (Methods in Molecular Biology). Available from: https://link.springer.com/https://doi.org/10.1007/978-1-0716-2772-3_18doi:10.1007/978-1-0716-2772-3_18.
30. Brinkmeyer-Langford C, Chu C, Balog-Alvarez C, Yu X, Cai JJ, Nabity M et al. Expression profiling of disease progression in canine model of Duchenne muscular dystrophy. Asakura A, editor. PLOS ONE. 2018;13(3):e0194485. https://doi.org/10.1371/journal.pone.0194485
31. Hildyard JCW, Riddell DO, Harron RCM, Rawson F, Foster EMA, Massey C, et al. The skeletal muscle phenotype of the DE50-MD dog model of Duchenne muscular dystrophy. Wellcome Open Res. 2022;7:238. https://doi.org/10.12688/wellcomeopenres.18251.1.
32. Nagano K. Quantitative analysis of approximate shapes in a myofiber cross-section and their relationship with myofiber cross-sectional area. J Phys Ther Sci. 2021;33(12):931–4. https://doi.org/10.1589/jpts.33.931.
33. Guo L, Soslow JH, Bettis AK, Nghiem PP, Cummings KJ, Lenox MW, et al. Natural History of Cardiomyopathy in Adult Dogs With Golden Retriever Muscular Dystrophy. J Am Heart Assoc. 2019;8(16):e012443. https://doi.org/10.1161/JAHA.119.012443.
34. Fine DM, Shin JH, Yue Y, Volkmann D, Leach SB, Smith BF, et al. Age-matched comparison reveals early electrocardiography and echocardiography changes in dystrophin-deficient dogs. Neuromuscul Disord. 2011;21(7):453–61. https://doi.org/10.1016/j.nmd.2011.03.010.
35. Pérez-López DO, Burke MJ, Hakim CH, Teixeira JA, Han J, Yue Y, et al. Circulatory CCL2 distinguishes Duchenne muscular dystrophy dogs. Dis Model Mech. 2025;18(3):dmm052137. https://doi.org/10.1242/dmm.052137.
36. Kharraz Y, Guerra J, Pessina P, Serrano AL, Muñoz-Cánoves P. Understanding the Process of Fibrosis in Duchenne Muscular Dystrophy. BioMed Res Int. 2014;2014:1–11. https://doi.org/10.1155/2014/965631.
37. Kodippili K, Rudnicki MA. Satellite cell contribution to disease pathology in Duchenne muscular dystrophy. Front Physiol. 2023;14:1180980. https://doi.org/10.3389/fphys. .2023.1180980 PubMed PMID: 37324396; PubMed Central PMCID: PMC10266354.
38. Riddell DO, Hildyard JCW, Harron RCM, Hornby NL, Wells DJ, Piercy RJ. Serum inflammatory cytokines as disease biomarkers in the DE50-MD dog model of Duchenne muscular dystrophy. Dis Model Mech. 2022;15(12):dmm049394. https://doi.org/10.1242/dmm.049394.
39. Villalta SA, Rinaldi C, Deng B, Liu G, Fedor B, Tidball JG. Interleukin-10 reduces the pathology of mdx muscular dystrophy by deactivating M1 macrophages and modulating macrophage phenotype. Hum Mol Genet. 2011;20(4):790–805. https://doi.org/10.1093/hmg/ddq523.
40. Kornegay JN, Bogan JR, Bogan DJ, Childers MK, Li J, Nghiem P, et al. Canine models of Duchenne muscular dystrophy and their use in therapeutic strategies. Mamm Genome. 2012;23(1–2):85–108. https://doi.org/10.1007/s00335-011-9382-y.
41. Duan D. Duchenne Muscular Dystrophy Gene Therapy in the Canine Model. Hum Gene Ther Clin Dev. 2015;26(1):57–69. https://doi.org/10.1089/humc.2015.006.
42. Morales ED, Wang D, Burke MJ, Han J, Devine DD, Zhang K, et al. Transcriptional changes of genes encoding sarcoplasmic reticulum calcium binding and up-taking proteins in normal and Duchenne muscular dystrophy dogs. BMC Musculoskelet Disord. 2024;25(1):811. https://doi.org/10.1186/s12891-024-07927-8.

Publisher's note Springer Nature remains neutral with regard to jurisdictional claims in published maps and institutional affiliations.

Authors and Affiliations

Shanti S. S. Rayagiri[1,3] · Johnathan K. Smid[1,3] · Phil Lambert[3] · James Jaquith[3] · Tessa Murray[3] · Ryan Mitchell[3] · Frank Gleeson[3] · Jacob G. Monast[1] · James A. Teixeira[4] · Yongping Yue[4] · Matthew J. Burke[4] · Gang Yao[5] · Dongsheng Duan[4,5,6,7] · Michael A. Rudnicki[1,2,3]

✉ Michael A. Rudnicki
mrudnicki@ohri.ca

1 Sprott Centre for Stem Cell Research, Regenerative Medicine Program, Ottawa Hospital Research Institute, Ottawa, Canada

2 Department of Medicine, Faculty of Medicine, University of Ottawa, Ottawa, Canada

3 Satellos Bioscience, Toronto, Canada

4 Department of Molecular Microbiology and Immunology, School of Medicine, University of Missouri, Columbia, MO, USA

5 Department of Chemical and Biomedical Engineering, College of Engineering, University of Missouri, Columbia, MO, USA

6 Department of Neurology, School of Medicine, University of Missouri, Columbia, MO, USA

7 Department of Pathobiology and Integrative Biomedical Sciences, College of Veterinary Medicine, University of Missouri, Columbia, MO, USA